

A 3D Bimodal (3,8)-connected Metal-organic Framework with **tfz-d** Topology Based on Tetranuclear Copper Clusters

Pei-juan Ma, Yue-Hua Li, Li Qin, and Guang-hua Cui*

College of Chemical Engineering, Hebei United University, 46 West Xinhua Road, Tangshan 063009, Hebei P.R. China

*E-mail: tscghua@126.com

Received August 19, 2013, Accepted September 3, 2013

Key Words : Cu(II) complex, Mixed ligand, Isonicotinate, **tfz-d** topology

During the past few decades, extensive endeavors have been focused on the rational design and controllable synthesis of metal-organic frameworks (MOFs) owing to their intriguing topologies and potential applications in gas storage, nonlinear optics, and catalysis.^{1,2} From the viewpoint of synthetic strategy of crystal engineering, the suitable selection of organic ligands and metal ions plays a dominating role on the construction of coordination polymers. In particular, the using polynuclear metal clusters as secondary building units (SBUs) are vital in constituting certain functional MOFs with seven-, eight-connected or highly connected topologies.³⁻⁵ In other hand, organic carboxylate groups can tightly aggregate two or more metal ions into a small molecular entity by its various coordination modes in the construction of coordination polymers, thus combining two rigid carboxylate ligands in which one is the pyridyl-containing ligand will be a useful strategy for the abundant and novel polymer architectures.⁶⁻¹¹ In continuation of our exploratory research toward developing a new family of MOFs based on polynuclear metal-clusters,¹² we presented the synthesis, crystal structure and catalytic properties of a 3D coordination framework $[\text{Cu}_2(\text{OH})(\text{ina})(\text{nip})_2]_n$ (nip = 5-nitroisophthalate, ina = isonicotinate), which shows a bimodal 3,8-connected **tfz-d** topology based on $[\text{Cu}_4(\mu_3\text{-OH})_2]_n$ clusters.

Experimental Section

Materials and Characterization Methods. All the solvents and reagents for synthesis were of analytical reagent grade and commercially available. Elemental analysis was performed on a Perkin-Elmer 240C analyzer. The IR spectrum was recorded in the 4000-400 cm^{-1} range using a FT-IR spectra with KBr pellets. Powder X-ray diffraction measurement was performed on a Rigaku D/Max-2500 diffractometer at 40 kV, 100 mA using Cu-K α radiation ($\lambda = 0.1542$ nm) in the 2θ range of 5-50° with a step size of 0.02° and a scanning rate of 10°/min. Thermogravimetric analysis (TGA) was collected on a NETZSCH TG 209 thermal analyzer from room temperature to 800 °C with a heating rate of 10 °C/min under nitrogen. The concentration of congo red solution was measured with a SHANGHAI JINGKE 722N spectrophotometer at maximum wavelength 496 nm.

Synthesis of $[\text{Cu}_2(\text{OH})(\text{ina})(\text{nip})]_n$. A mixture of $\text{CuCl}_2 \cdot 6\text{H}_2\text{O}$ (0.2 mmol, 34 mg), H_2nip (0.15 mmol, 32 mg), Hina (0.1 mmol, 12 mg), NaOH (0.24 mmol, 10 mg) and H_2O (16 mL) was placed in a Teflon-lined stainless steel vessel. The mixture was sealed and heated at 140 °C for 3 days under autogenous pressure. When the sample was cooled to room temperature at a rate of 5 °C/h, blue block-shaped crystals were collected in 24.7% yield (based on Cu). Anal. calcd for $\text{C}_{14}\text{H}_8\text{Cu}_2\text{N}_2\text{O}_9$ ($M_r = 475.32$): C, 35.38; H, 1.70; N, 5.89. Found: C, 35.12; H, 1.55; N, 5.62. IR (KBr pellet, v/cm^{-1}) ν 3470s, 3097m, 1617s, 1550s, 1513m, 1442s, 1280m, 1060s, 913w, 727s, 469m.

Catalytic Experiments. The catalytic degradation of azo dye was operated in a 250 mL three-necked flask reactor with magnetic stirring. The reaction temperature was controlled by circulating constant at 30 °C. The complex (20 mg) firstly was mixed with 200 mg/L congo red solution in the reactor. When the temperature was stable, the reaction was initiated by adding 0.5 mL 30% (w/w) H_2O_2 to the above mixture. At given time intervals, 3.0 mL solution was taken out and centrifuged to remove the residual catalyst, then analyzed with a UV-Vis spectrophotometer at an absorption wavelength of 496 nm. This procedure was also repeated in the absence of catalyst as a control experiment under the same condition. The degradation efficiency of congo red is defined as follows:¹³

$$\text{Degradation efficiency} = (C_0 - C) / C_0 \times 100\% \quad (1)$$

Where C_0 (mg/L) is the initial concentration of congo red, and C (mg/L) is the concentration of congo red at reaction time, t (min).

Crystallography. X-ray single-crystal diffraction data of the complex was collected on a Bruker Smart 1000 CCD diffractometer using graphite-monochromated Mo-K α radiation ($\lambda = 0.71073$ Å) at room temperature with ω -2 θ scan mode. A semi-empirical absorption correction was applied using the SADABS program.¹⁴ The structure was solved using direct methods and refined by full-matrix least-squares by SHELXTL program package.¹⁵ The Cu atom in the complex was located from the E-maps, and other non-hydrogen atoms were located in successive difference Fourier syntheses and refined with anisotropic displacement parameters on F^2 . The hydrogen atoms of the organic ligands

were generated theoretically onto the specific atoms and refined isotropically. CCDC-941799 contains the supplementary crystallographic data. The crystallographic data for the complex is summarized in Table S1, and the selected bond lengths and angles are listed in Table S2 (Supporting Information).

Results and Discussion

The complex crystallizes in the triclinic system with $P\bar{1}$ space group. The asymmetric unit of the complex consists of two crystallographically independent copper atoms, one μ_3 -OH group, one ina and one nip ligands. As shown in Figure 1, the coordination geometry of two copper centers can be considered as a square pyramidal due to the τ_5 value being 0.17 for Cu1 atom, 0.11 for Cu2 atom.¹⁶ The Cu1 atom is five-coordinated by two oxygen atoms from two different nip ligands, one μ_3 -OH group, one pyridyl nitrogen atom and one oxygen atom from two distinct ina ligands; the Cu2 atom is surrounded by two oxygen atoms from two nip ligands, two μ_3 -OH groups and one oxygen atom from one ina ligand. All the bond lengths and angles around copper centers are in the range of reported values,¹⁷ and the selected bonds and angles are listed in Table S2. The nip ligand displays a μ_4 - $\eta^1, \eta^1, \eta^1, \eta^1$ coordination mode and the ina anion adopts a tridentate bridging μ_3 - η^1, η^1, η^1 coordination fashion. It is interesting to note that the complex contains $[\text{Cu}_4(\mu_3\text{-OH})_2]$ tetranuclear clusters. Its center of inversion is situated in the middle of the two μ_3 -OH groups, and four neighboring Cu atoms lie on an absolute plane to form an approximate parallelogram, in which the Cu1...Cu1B and Cu2...Cu2B (symmetry codes: B = $-x+1, -y, -z+1$) distances are 5.8746(2) and 2.9564(2) Å, respectively. The two sides of the parallelogram are unequal with the Cu1...Cu2B and Cu1...Cu2 separations of 3.3848(13) and 3.1889(13) Å, respectively. In the crystal structure complex, $[\text{Cu}_4(\mu_3\text{-OH})_2]$ clusters are linked by neighbor six ina ligand to form an infinite 2D sheet parallel to ac plane, then these adjacent layers are further pillared by accessorial nip ligands with its carboxylate groups to generate a 3D coordination framework. Topologically, each $[\text{Cu}_4(\mu_3\text{-OH})_2]$ SBU is linked by eight neighbour ones and can be act as a 8-connected node (Figure 2), each ina⁻ ligand is connected to three equivalent $[\text{Cu}_4(\mu_3\text{-OH})_2]$ SBUs to act as a 3-connected node, and nip ligands are viewed as ditopic linkers. The succeeding topology analysis by TOPOS 4.0 program suggests the coordination framework can be simplified as a bimodal (3,8)-connected nets with **tfz-d** topology,¹⁸ a point symbol of $(4^3)_2(4^6.6^{18}.8^4)$ (Figure 3).¹⁹ Compared with the other reported **tfz-d** frameworks,²⁰ this bimodal 3D network represents the first example of a metal-organic framework with **tfz-d** topology based on tetranuclear copper clusters. The net in this complex provides a novel example and demonstrates that the tetranuclear $[\text{Cu}_4(\mu_3\text{-OH})_2]$ SBU is effective in the construction of bimodal highly-connected network. The driving force of the topology-construction may be from strict requirements on ligand functionalities and more complicated

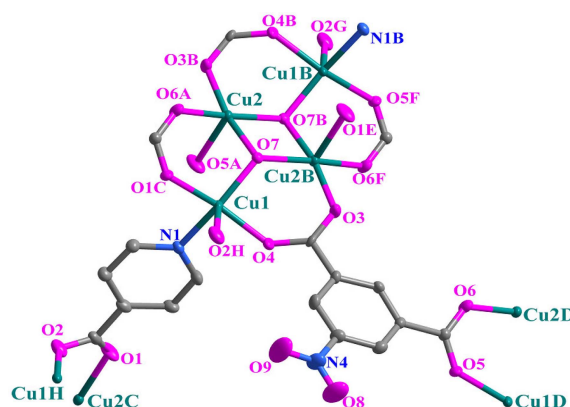


Figure 1. The coordination environments of Cu centers and tetranuclear clusters in the complex. Symmetry codes: A = $x, y-1, z$; B = $-x+1, -y, -z+1$; C = $-x+1, -y, -z$; D = $x, y+1, z$; E = $x, y, z+1$; F = $-x+1, -y+1, -z+1$; G = $-x+1, y, z+1$; H = $2-x, -y, -z$.

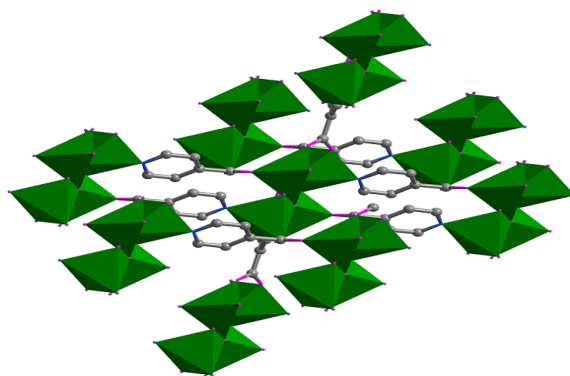


Figure 2. View of the 8-connected $[\text{Cu}_4(\mu_3\text{-OH})_2]$ SBU in the complex, depicting the connections to eight neighbour ones.

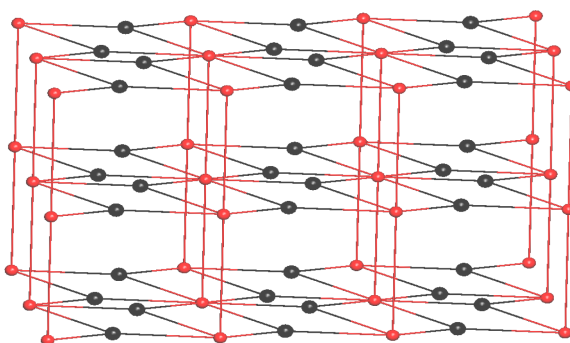


Figure 3. The **tfz-d** topology network of the complex. The red and black spheres represent the tetranuclear copper clusters and ina ligand, respectively.

geometry principles.^{11a}

In the FT-IR spectrum of the complex, the asymmetric and symmetric stretching vibrations of the carboxylate groups are observed at 1610–1389 cm^{-1} for nip and ina ligands. There is a broad band at 3470 cm^{-1} may be assigned to the stretching vibrations $\nu(\text{OH})$ of OH group. The characteristic band at 1550 cm^{-1} is related to the nitro group of nip anions.

Simulated and experimental powder X-ray diffraction (PXRD) patterns of the compound are shown in Figure S1

(Supporting Information). All the peak positions of the simulated and experimental PXRD patterns are in agreement with each other, demonstrating clearly the good phase purity of the as-prepared products.

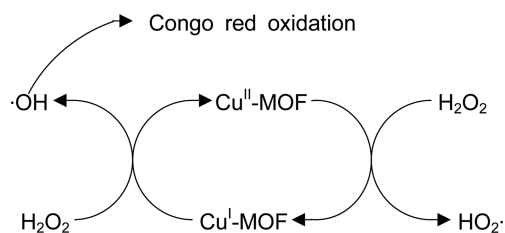
The thermogravimetric analysis (TGA) of powder sample was carried out from 20 to 800 °C under nitrogen atmosphere at the heating rate of 10 °C/min, as shown in Figure S2. The 3D framework is stable up to 330 °C, and then an abrupt weight loss occurs. The TGA data analysis indicates this complex keeps a relatively high thermal stability.

Congo red (sodium salt of benzidinediazo-bis-1-naphthylamine-4 sulfonic acid) is one of the important azo dyes, used for coloring of paper products and unaffected by conventional treatment systems for degradation. Recently, much attention has been focused on the heterogeneous Fenton and Fenton-like reactions to oxidize contaminants of concern such as azo dyes, which largely depend on transition metal-based catalysts. In particular, the development of metal-organic frameworks into catalysts could yield several significant advantages, such as enhancing catalyst stability due to the spatial separation of individual catalytic sites in the framework, high catalytic activity, better selectivity, and ease of separability.²¹ In addition, hydrogen peroxide (H₂O₂) is a precursor of hydroxyl radicals, which can degrade and mineralize azo dye molecules in water.^{22,23}

The degradation experiments of congo red by hydrogen peroxide activated with the complex were investigated. As shown in Figure 4, the degradation efficiencies of congo red are fast within 5 min and achieved 88.72% with the complex as catalyst. The rate of the catalytic reaction increased quickly in 5 min, there after congo red oxidation proceeded in a gradual manner, in which degradation efficiencies were up to 97.93% after 110 min. However, without catalyst, the degradation efficiency of a control experiment was very low with only 9.70% after 110 min. In contrast with similar catalyst,²⁴ the complex has a remarkable achievement on degradation of congo red. The catalytic activities may be due to their distinct polynuclear metal clusters structures.

Based on the experimental observations, the mode of action of the catalysis was suggested utilizing the redox properties of H₂O₂ in Fenton process.²⁵ (Scheme 1):

In summary, we have synthesized and characterized a new three-dimensional coordination framework with bimodal 3,8-connected **tfz-d** topology based on tetranuclear copper clusters. Furthermore, the complex exhibits high activity in the Fenton-like reaction for the degradation of congo red.



Scheme 1. Schematic representation of catalysis reaction of the complex.

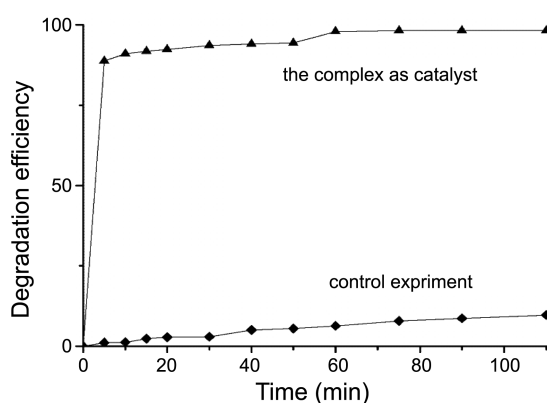


Figure 4. The experiment results of the catalytic degradation of congo red.

Supplementary Material. CCDC number: 941799 for the complex. The data can be obtained free of charge via https://services.ccdc.cam.ac.uk/structure_deposit (or from the Cambridge Cryst allographic Data Centre, 12, Union Road, Cambridge CB21EZ, UK; fax: (44)1223-336-033(44); or deposit@ccdc.cam.ac.uk).

Acknowledgments. The publication cost of this paper was supported by the Korean Chemical Society.

References

- (a) Furukawa, H.; Cordova, K. E.; O'Keeffe, M.; Yaghi, O. M. *Science* **2013**, *341*, 1230444-1. (b) Zhou, H. C.; Long, J. R.; Yaghi, O. M. *Chem. Rev.* **2012**, *112*, 673. (c) Wang, C.; Zhang, T.; Lin, W. B. *Chem. Rev.* **2012**, *112*, 1084. (d) Li, J. R.; Sculley, J. L.; Zhou, H. C. *Chem. Rev.* **2012**, *112*, 869. (e) Cook, T. R.; Zheng, Y. R.; Stang, P. J. *Chem. Rev.* **2013**, *113*, 734.
- (a) Du, M.; Li, C. P.; Liu, C. S.; Fang, S. M. *Coord. Chem. Rev.* **2013**, *257*, 1282. (b) Ulrich, S. *Chem. Soc. Rev.* **2011**, *40*, 575. (c) Dhakshinamoorthy, A.; Alvaro, M.; Garcia, H. *Catal. Sci. Technol.* **2011**, *1*, 856.
- (a) Cao, H. Y.; Liu, Q. Y.; Liu, C. M.; Wang, Y. L.; Chen, L. L.; Xiong, L. H. *Inorg. Chem. Commun.* **2013**, *34*, 12. (b) O'Keeffe, M.; Yaghi, O. M. *Chem. Rev.* **2012**, *112*, 675.
- Kostakis, G. E.; Ako, A. M.; Powell, A. K. *Chem. Soc. Rev.* **2010**, *39*, 2238.
- (a) Luo, F.; Che, Y. X.; Zheng, J. M. *Cryst. Growth Des.* **2009**, *9*, 1066. (b) Xu, Y.; Luo, F.; Che, Y. X.; Zheng, J. M. *Inorg. Chem. Commun.* **2009**, *12*, 639.
- Wang, H. S.; Ma, J. G.; Zhai, B.; Liu, Y. Y.; Cheng, P. *J. Mol. Struct.* **2007**, *829*, 1.
- Zhang, J.; Kang, Y.; Zhang, J.; Li, Z. J.; Qin, Y. Y.; Yao, Y. G. *Eur. J. Inorg. Chem.* **2006**, *2006*, 2253.
- (a) Zhao, F. H.; Che, Y. X.; Zheng, J. M. *Inorg. Chem. Commun.* **2012**, *16*, 55. (b) Tao, T.; Wang, X. X.; Wang, Y. N.; Lu, Z. Y.; Huang, W. *Inorg. Chem. Commun.* **2013**, *31*, 62.
- Zhu, X. F.; Wang, N.; Luo, Y. H.; Pang, Y.; Tian, D.; Zhang, H. *Aust. J. Chem.* **2011**, *64*, 1346.
- (a) Zhong, C. B.; Feng, X. F.; Tian, X. Z.; Zhu, Y.; Sun, G. M.; Song, Y. M.; Luo, F. *Inorg. Chem. Commun.* **2012**, *26*, 17. (b) Zhao, D.; Timmons, D. J.; Yuan, D. Q.; Zhou, H. C. *Acc. Chem. Res.* **2011**, *2*, 123. (c) O'Keeffe, M.; Eddaoudi, M.; Li, H. L.; Reinecke, T.; Yaghi, O. M. *J. Solid State Chem.* **2000**, *152*, 3.
- (a) Zhang, Y. B.; Zhang, J. P. *Pure Appl. Chem.* **2013**, *85*, 405. (b) Li, J.; Ji, C. C.; Lu, Z. Z.; Wang, T. W.; Song, Y.; Li, Y. Z.; Zheng, H. G.; Guo, Z. J.; Batten, S. R. *CrystEngComm* **2012**, *12*, 4424.

12. (a) Xiao, S. L.; Cui, G. H.; Blatov, V. A.; Geng, J. C.; Li, G. Y. *Bull. Korean Chem. Soc.* **2013**, *34*, 1891. (b) Zhang, W. G.; Cui, G. H.; Xiao, S. L.; Du, X. *Bull. Korean Chem. Soc.* **2013**, *34*, 1243.
 13. Qin, L.; Zheng, J.; Xiao, S. L.; Zheng, X. H.; Cui, G. H. *Inorg. Chem. Commun.* **2013**, *34*, 71.
 14. Sheldrick, G. M. SADABS (version 2.03), *Program for Empirical Absorption Correction of Area Detector Data*, University of Göttingen, Göttingen (Germany), 1996.
 15. Sheldrick, G. M. *Acta Crystallogr.* **2008**, *A64*, 112.
 16. Addison, A. W.; Rao, T. N.; Reedijk, J.; Van-Rijn, J.; Verschoor, G. C. *Dalton Trans.* **1984**, 1349.
 17. Huh, H. S.; Lee, S. W. *J. Mol. Struct.* **2007**, *829*, 44.
 18. Blatov, V. A. *Struct. Chem.* **2012**, *23*, 955.
 19. Blatov, V. A.; O'Keeffe, M.; Proserpio, D. M. *CrystEngComm* **2010**, *12*, 44.
 20. (a) Cui, J. H.; Li, Y. Z.; Guo, Z. J.; Zheng, H. G. *Chem. Commun.* **2013**, *49*, 555. (b) Luo, F.; Che, Y. X.; Zheng, J. M. *Cryst. Growth Des.* **2008**, *8*, 2006. (c) Chen, S. S.; Bai, Z. S.; Fan, J.; Lv, G. C.; Su, Z.; Sun, W. Y. *CrystEngComm* **2010**, *12*, 3091. (d) Xu, G. J.; Zhao, Y. H.; Shao, K. Z.; Lan, Y. Q.; Wang, X. L.; Su, Z. M.; Yan, L. K. *CrystEngComm* **2009**, *11*, 1842. (e) Liu, Z. Y.; Chu, J.; Ding, B.; Zhao, X. J.; Yang, E. C. *Inorg. Chem. Commun.* **2011**, *14*, 925.
 21. Jiao, C. H.; He, C. H.; Geng, J. C.; Cui, G. H. *Transition Met. Chem.* **2012**, *37*, 17.
 22. Geng, J. C.; Qin, L.; Du, X.; Xiao, S. L.; Cui, G. H. *Z. Anorg. Allg. Chem.* **2012**, *638*, 1233.
 23. Ramirez, J. H.; Duarte, F. M.; Martins, F. G.; Costa, C. A.; Madeira, L. M. *Chem. Eng. J.* **2009**, *148*, 394.
 24. Cui, G. H.; He, C. H.; Jiao, C. H.; Geng, J. C. *CrystEngComm* **2012**, *14*, 4210.
 25. Etaiw, S. E. H.; Amer, S. A.; El-Bendary, M. M. *J. Inorg. Organomet. Polym.* **2011**, *21*, 662.
-